nature physics

ARTICLES

PUBLISHED ONLINE: 22 MAY 2011 | DOI: 10.1038/NPHYS2002

Quantifying how DNA stretches, melts and changes twist under tension

Peter Gross[1], Niels Laurens[1], Lene B. Oddershede[2], Ulrich Bockelmann[3], Erwin J. G. Peterman[1]*† and Gijs J. L. Wuite[1]*†

In cells, DNA is constantly twisted, bent and stretched by numerous proteins mediating genome transactions. Understanding these essential biological processes requires in-depth knowledge of how DNA complies to mechanical stress. Two important physical features of DNA, helical structure and sequence, are not incorporated in current descriptions of DNA elasticity. Here we connect well-defined force–extension measurements with a new model for DNA elasticity: the twistable worm-like chain, in which DNA is considered a helical, elastic entity that complies to tension by extending and twisting. In addition, we reveal hitherto unnoticed stick–slip dynamics during DNA overstretching at ∼65 pN, caused by the loss of base-pairing interactions. An equilibrium thermodynamic model solely based on DNA sequence and elasticity is presented, which captures the full complexity of this transition. These results offer deep quantitative insight in the physical properties of DNA and present a new standard description of DNA mechanics.

Over the past two decades, much effort has been devoted to obtaining a complete picture of the mechanics of DNA. For mechanical loads below ∼35 pN, double-stranded (ds)DNA extensibility and bending rigidity is described well by the extensible worm-like chain (WLC) model[1–4], a model that regards DNA as a homogeneous, extensible rod. However, the double-helical structure and base-pairing interactions, important structural aspects of dsDNA, are not taken into account, which might be the reason the WLC-model fails to describe DNA elasticity at intermediate and higher forces. A recent experiment demonstrated that DNA extension cannot be considered separately from twist, as these two elastic parameters are intricately coupled[5]. How this twist–stretch coupling affects the elasticity of DNA is unclear. Another striking feature of DNA elasticity is the overstretching transition, occurring at 65 pN, resulting in a 70% increase of DNA length[3,6]. The molecular details of this transition are still under debate. Initially it was argued that DNA adopts an unwound but base-paired structure[6,7]. An alternative view emerged from experiments on the thermodynamics of DNA overstretching, suggesting that the base-pairing interactions gradually dissolve during this transition[8,9]. This interpretation gained further support from experiments that studied the effect of single-stranded DNA-specific ligands[10]. Recently we observed directly that at the overstretching tension the two strands indeed unpeel[11]. As the DNA sequence composition determines the interaction energy of the two hybridized DNA strands, a strong sequence dependence on the force-induced DNA unpeeling is expected. So far, however, a clear effect of local sequence on the energetics of force-induced unpeeling has remained elusive. Here we measure the elastic properties of DNA with unprecedented resolution to obtain a complete mathematical model of DNA elasticity, including the overstretching transition, taking into account sequence composition and a force-dependent twist–stretch coupling.

To address the sequence dependence of the unpeeling process, we generated a DNA-construct with only one free DNA end, such that unpeeling can initiate exclusively at one location, and proceed in only one direction (see Methods; Fig. 1a). This DNA-construct was connected to two optically trapped, streptavidin-coated microspheres[12]. We stretched the DNA to about 65 pN and monitored the generation of single-stranded (ss)DNA with fluorescence microscopy using enhanced green fluorescent protein (eGFP)-tagged Replication Protein A (RPA) as the ssDNA reporter[11]. For all DNA molecules tested ($N = 20$) overstretching resulted in the formation of ssDNA through a single unpeeling front (Fig. 1b). High-resolution force–extension curves of such DNA constructs show two marked features (Fig. 1c): (1) the force–extension curves deviate substantially from the extensible WLC model above ∼35 pN (Fig. 1c, regime I), and (2) at forces above 60 pN overstretching sets in, not as a smooth transition, but with a distinct saw-tooth pattern (Fig. 1c, regime II).

From regime I it becomes clear that the extensible WLC model overlooks important aspects of DNA elasticity that become relevant at intermediate forces. We hypothesized that inclusion of the mechanical coupling between extension and twist of the double helix[13,14] is imperative. Such a twist–stretch coupling term must be considered in a consistent linear theory of a chiral polymer[15]. In experiments, the twist–stretch relation has been shown to depend on force in a complex way: at low forces DNA overwinds when stretched, at forces above 35 pN it unwinds[5]. Consequently, torsionally unconstrained DNA will comply to an external force in two ways: by stretching, and by overwinding or unwinding. We thus incorporated an enthalpic term capturing the elongation of DNA due to changes in twist into the extensible WLC model. This linear 'twistable worm-like chain' model (tWLC) yields the following relation between extension (x) and force (F) (see Supplementary Information):

$$x = L_c\left(1 - \frac{1}{2}\sqrt{\frac{k_B T}{F \cdot L_p}} + \frac{C}{-g(F)^2 + SC}\cdot F\right) \qquad (1)$$

[1]LaserLaB Amsterdam and Department of Physics and Astronomy, VU University, De Boelelaan 1081, 1081 HV, Amsterdam, The Netherlands, [2]Niels Bohr Institute, Blegdamsvej 17, 2100 Copenhagen, Denmark, [3]Laboratoire Nanobiophysique, ESPCI, CNRS UMR Gulliver 7083, 10 rue Vauquelin 75005, Paris, France. †These authors contributed equally to this work. *e-mail: erwinp@nat.vu.nl; gwuite@nat.vu.nl.

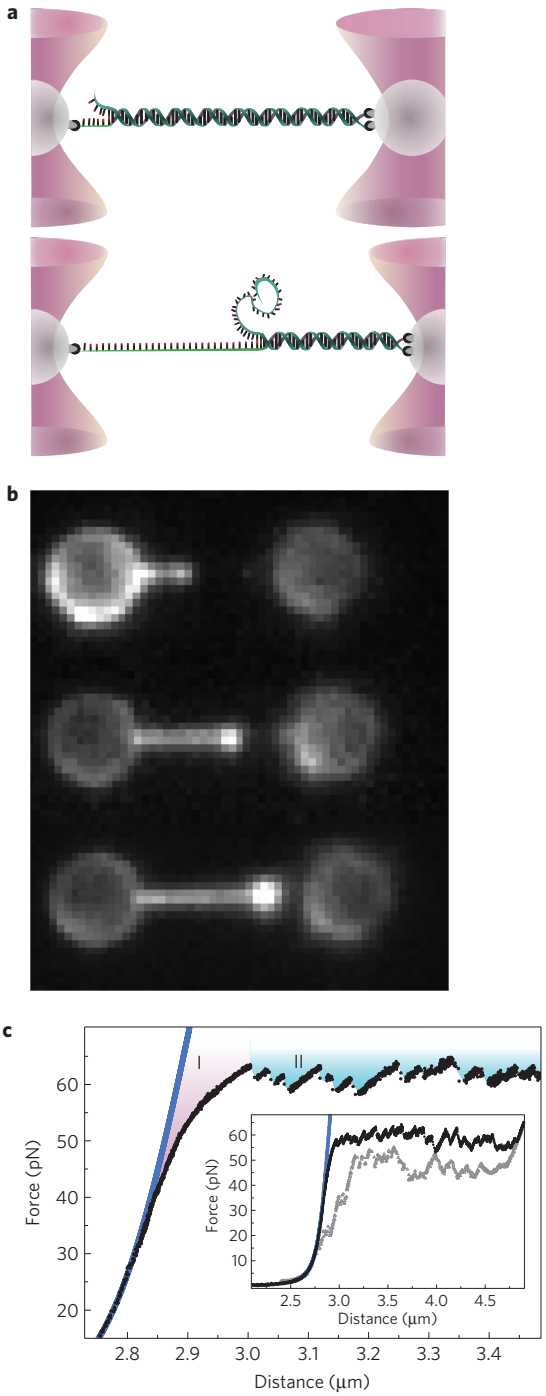

Figure 1 | Force-induced strand unpeeling of DNA studied with fluorescence microscopy and force spectroscopy. a, Schematic depictions of the DNA construct used in this study undergoing unpeeling on extension. Three ends of the DNA strands are connected to the optically trapped microspheres. **b**, Three fluorescence images of partially overstretched DNA molecules. After partial overstretching, the DNA molecules are exposed to 20 nM fluorescently labelled single-stranded binding protein eGFP–RPA in a buffer containing up to 150 mM NaCl (50 mM shown here). Only the left part of the DNA construct is fluorescent, indicating unpeeling has occurred only from the left side of the DNA. **c**, Force–extension measurement of a DNA construct like that shown in **a**. In region I, a strong deviation from the extensible WLC (blue line) is evident. In region II, the overstretching transition, pronounced step-wise increases in contour length can be discerned. Inset: extended view of the same experimental curve (black), together with the reverse process, strand reannealing on relaxation (grey).

Here, DNA is parameterized by: the contour length L_c, the twist rigidity C, the stretching modulus S, the persistence length L_p (refs 2,3,16), and the twist–stretch coupling $g(F)$ (refs 5, 17,18). We followed two approaches to obtain insight into the functional form of the force dependence of the twist–stretch coupling. Using the tWLC model, which connects the state of extension to the state of unwinding or overwinding, $g(F)$ was determined (1) from our force–extension measurements and (2) from the force-unwinding/overwinding measurements conducted by Gore *et al.* (ref. 5). To determine $g(F)$ from force–extension measurements, we solved equation (1) for $g(F)^2$ (Supplementary Eq. S5). Using this equation, the force dependence of the twist–stretch coupling (Fig. 2a, open circles) is obtained from the experimental force–extension curves (Fig. 2b), taking the twist rigidity C from the literature[16], and values for the persistence length L_p, the contour length L_c and stretching modulus S from an extensible WLC fit to the same measurement ($<$35 pN, Fig. 2b). Alternatively, by applying Supplementary Eq. S3 to the measurements of Gore *et al.* of the force-dependence of the winding state, we can also gain access to the force-dependence of the twist–stretch coupling (Fig. 2a, black line). Figure 2a shows that both approaches for the determination of $g(F)$ converge to a statistically indistinguishable force-dependence of the twist–stretch coupling (see also Supplementary Information). For forces below $\sim$30 pN, $g(F)$ is negative and constant, with a value of ~ -100 pN nm, in agreement with magnetic tweezers studies[5,17,18]. For forces higher than 30 pN, the twist–stretch coupling rises monotonically, until it changes sign at $\sim$35 pN, where DNA starts to unwind[5]. In an approach opting for simplicity we describe $g(F)$ as constant at forces below F_c, whereas the high-force regime is approximated to linear order: $g_0 + g_1 F$ (Supplementary Information). From force–extension measurements we obtain: $g_0 = -590 \pm 50$ pN nm, $g_1 = 18 \pm 0.5$ nm and $F_c = 30 \pm 4$ pN ($N = 7$; errors are standard errors of the means), and the fit to $g(F)$ from overwinding/unwinding measurements[5], shown in Fig. 2a, yields nearly identical values (See also Supplementary Information). Incorporation of this functional form of $g(F)$ into the tWLC-model results in a substantially improved description of DNA elasticity, up to the onset of the overstretching transition (Fig. 2b). Fits of the tWLC model to force–extension curves of the $\sim$6 times longer lambda DNA yielded virtually identical results (Supplementary Fig. S1, $g_0 = -560 \pm 20$ pN nm, $g_1 = 18 \pm 1$ nm, $F_c = 30 \pm 1$ pN. $N = 7$, errors represent standard errors of the means), indicating that $g(F)$ is independent of DNA length and sequence, in agreement with ref. 18. Finally, we evaluated what this functional form of the $g(F)$ implies for changes in the twist of extended DNA (Supplementary Eq. S3). Figure 2c shows the calculated change in DNA twist using the elastic parameters obtained from a tWLC fit to force–extension measurement compared to the overwinding/unwinding data of Gore *et al.* (ref. 5). The ability of the tWLC model to successfully describe, at the same time, force–extension and force–twist experiments highlights that the introduction of the force-dependent twist–stretch coupling correctly quantifies how DNA complies to tension. A complex force dependence of the twist–stretch coupling has been obtained from molecular modelling calculations[18], albeit in the low-force regime. More theoretical and experimental effort is needed to provide a molecular basis for the non-trivial behaviour observed here. Notably, the results of Fig. 2c reveal that the total amount of unwinding due to tension is limited: only $\sim$3% of the total twist is lost on stretching up to the onset of the overstretching transition. The implication of this finding is that significant forces are required to induce DNA unwinding by tension. In cells, where DNA is continuously subject to thermal and protein-induced tension, this robustness of the helical structure might be important for reliable sequence recognition by minor- or major-groove binding proteins.

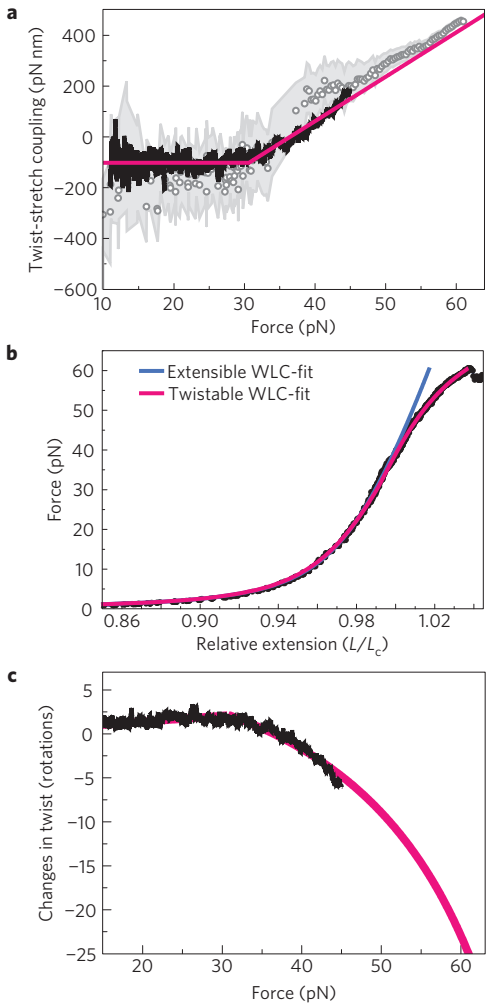

Figure 2 | DNA unwinding under tension quantified using the twistable worm-like chain (tWLC) model. a, Force dependence of the twist–stretch coupling. Black line: Twist–stretch coupling deducted from measurements of the change in DNA twist on increasing tension[5], calculated with the tWLC model (Supplementary Information, Eq. S3). We used the following parameters: $L_c = 2.87\,\mu$m, $S = 1{,}500$ pN, $C = 440$ pN nm^2 (refs 5,16). Red line: Fit of the phenomenological Supplementary Eq. S3, yielding: $g_0 = -637$ pN nm, $g_1 = 17$ nm and $F_c = 30.6$ pN. Grey dots: determination of the twist–stretch coupling from a typical force–extension measurement, using the twistable worm-like chain (Supplementary Eq. S5) with an error band determined from a propagation of uncertainty in force ($\Delta F \approx 0.2$ pN) and extension ($\Delta x \approx 5$ nm). **b**, Comparison of the extensible WLC model with the twistable WLC model. Black dots: Force–extension measurement. Red curve: Fit of the tWLC in the force range 1.5–60 pN, with a twist–stretch coupling from **a** ($g_0 = -637$ pN nm, $g_1 = 17$ nm, $F_c = 30.6$ pN) and fitted parameters $L_c = 2.85\,\mu$m, $S = 1{,}430$ pN and $L_p = 40$ nm. (Ensemble average ($N = 7$) and standard error of the mean: $L_c = 2.85 \pm 0.005\,\mu$m, $S = 1{,}450 \pm 50$ pN, $L_p = 38 \pm 2$ nm.) Blue curve: fit of the extensible WLC model in the force range 1.5–35 pN: $L_p = 38.7$ nm, $L_c = 2.86\,\mu$m and $S = 1{,}540$ pN (ensemble average ($N = 7$) and standard error of the mean: $L_c = 2.85 \pm 0.006\,\mu$m, $S = 1{,}600 \pm 120$ pN, $L_p = 39 \pm 3$ nm.) **c**, Change in twist of a 8.4 kb DNA construct as a function of tension. Black line: Measured data by Gore *et al.* (ref. 5). Red line: Force-induced changes in twist, calculated with the twistable worm-like chain model (Supplementary Eq. S3), using $g(F)$ from **a**, along with the elastic parameters: $C = 440$ pN nm^2, $L_c = 2.87\,\mu$m, $S = 1{,}500$ pN (refs 5,16).

Regime II in Fig. 1b shows DNA overstretching[3,11]. At pulling speeds of 10 nm s^{-1}, force–extension curves display a clear

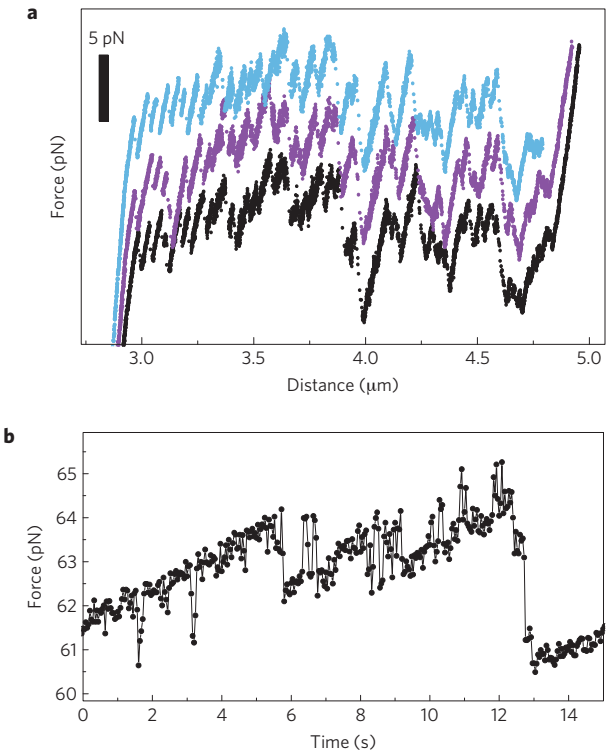

Figure 3 | Stick–slip dynamics are sequence-dependent and close to equilibrium. a, Stick–slip melting of three different dsDNA molecules with identical sequence shows reproducible patterns. The curves are offset for visibility. **b**, Dynamics of burst-wise melting (extension rate, 10 nm s^{-1}; sampling frequency, 23 Hz). Bistable behaviour is apparent close to the critical force of melting events.

saw-tooth-like pattern (Fig. 3a), suggesting that force-induced unpeeling proceeds in a burst-like manner. Similar molecular 'stick–slip' dynamics have been observed in dsDNA unzipping experiments, where tension is applied to both strands on one side of a dsDNA template[19–21]. In that configuration, 15 pN is needed to separate the two strands, approximately four times lower than required for overstretching, which can be understood by realizing that the gain in contour length obtained per melted base pair differs by a factor of four between the two experimental geometries (unzipping: $2 \cdot L_{\mathrm{bp,ssDNA}} \approx 1$ nm versus overstretching: $L_{\mathrm{bp,ssDNA}} - L_{\mathrm{bp,dsDNA}} \approx 0.25$ nm; ref. 22). In the unzipping geometry the stick–slip dynamics depend on the base-pairing energy and thus the DNA sequence[19,20]. Similarly, we observed that in the overstretching geometry the complex stick–slip pattern is very similar for different DNA molecules with identical sequence ($N = 17$; Fig. 3a), indicating that this pattern directly reflects the sequence-specific base-pairing energy landscape. The situation is different when unpeeling can occur from two (or more) fronts. In an attachment geometry allowing two unpeeling fronts, stick–slip features are still observed (Supplementary Fig. S2A). The patterns, however, vary substantially between experiments and molecules, as a result of the many alternative unpeeling pathways.

Next, we examined whether DNA unpeeling occurs close to equilibrium. Reproducible, deterministic stick–slip dynamics were observed at extension velocities up to 20 nm s^{-1} (Supplementary Figs S3 and S2B), as expected for a process close to equilibrium. In addition, we observed bistable, repetitive transitions of multiple base pairs opening and closing, close to the critical force of individual melting events (Fig. 3b; Supplementary Fig. S4), similar to force-induced RNA hairpin[23,24] and DNA unzipping

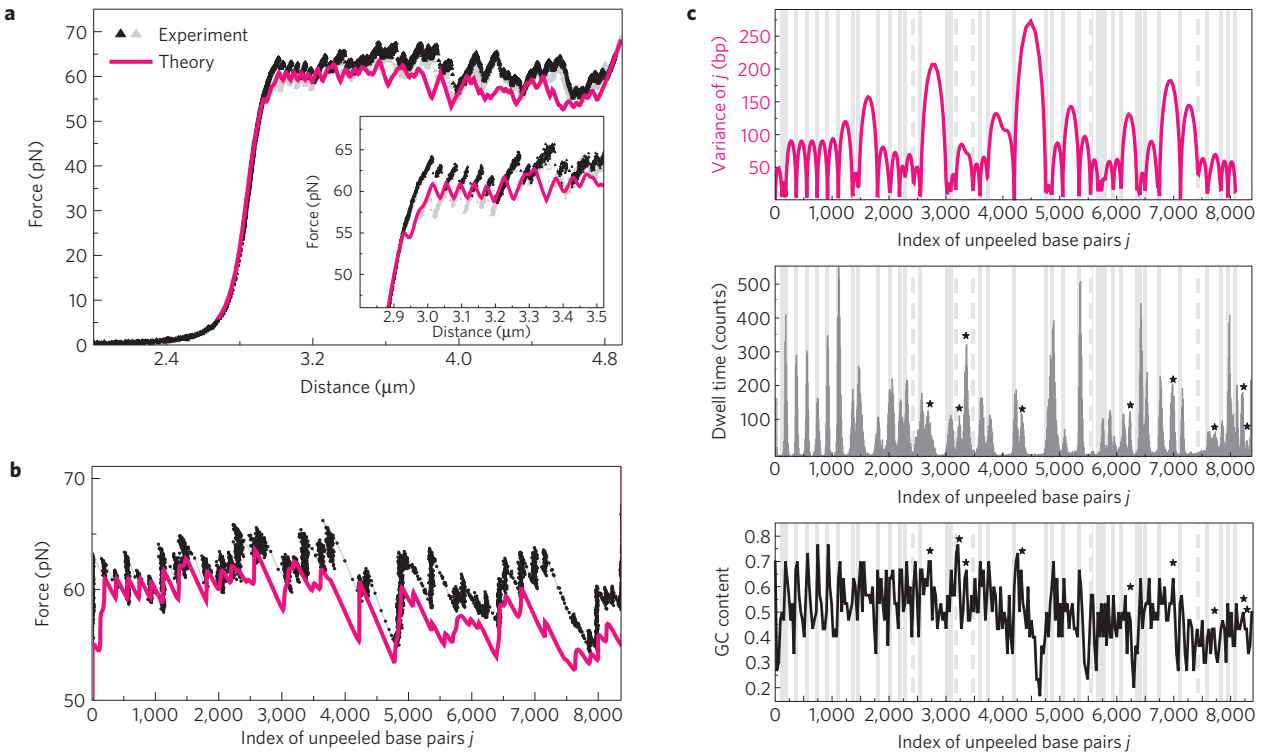

Figure 4 | Modelling of force-induced, sequence-specific unpeeling of dsDNA. a, Force–extension curves of DNA molecules with identical sequence. Grey and black, data (extension speed, 10 nm s^{-1}); red, equilibrium model (see text for details). The inset shows the start of the unpeeling process. **b**, Comparison of measured (black) and calculated (red) force as function of unpeeling progress. Here the assumption is made that the mechanical properties of a partly unpeeled DNA molecule are a linear combination of those of dsDNA and ssDNA. **c**, Comparison of the measured (middle) and calculated (top) stalling locations of the unpeeling process. Middle panel: dwell-time histogram obtained from 12 independent force–extension curves of different DNA molecules with identical sequence (extension speed, 10 nm s^{-1}). Individual force–extension curves were converted to force against number of unpeeled base pairs. Histograms of the number of data points at a given unpeeling state were calculated and summed with a bin width of 9 bp. Top panel: variance of the position of the unpeeling front j versus its position as calculated from our equilibrium model (Supplementary Eq. S9). Grey vertical lines highlight the predicted stalling locations from this calculation (var(j) < 40 bp). The width of these grey bars represents the resolution limit of the position of the unpeeling front (~40 bp). Discontinuous grey bars indicate the location of predicted stalling locations where the dwell-time histogram shows only a very transient arrest of the unpeeling progress. Stars indicate stalling locations in a large melting burst (>300 bp) that are not captured by the model. Lower panel: GC content of the investigated pKYB1 DNA construct is displayed, from $j = 0$ (first base that unpeels) to $j = 8{,}389$, using a binning window of 30 base pairs.

experiments[21]. This provides additional evidence that burst-wise melting occurs close to equilibrium.

To quantitatively understand the force-induced DNA melting process, we adapted a statistical physics description of mechanical DNA unzipping[20,21]. In this model, the state of the DNA molecule is characterized by the number of unpeeled base pairs j and the lengths of the dsDNA, l_{ds}, and ssDNA, l_{ss}, segments. The free energy is calculated by summing four energy terms: (1) The free energy change of unpeeling base pair 1 to base pair j, $E_{bp}(j)$. This term depends on the DNA sequence and is determined using the nearest-neighbour model of SantaLucia for base-pairing[25]. (2) The elastic energy of the ssDNA fraction of j bases stretched to a length l_{ss}, $E_{ssDNA}(j, l_{ss})$, calculated using the freely jointed chain model[3]. (3) The elastic energy of the dsDNA segment of j_{tot}–j base pairs stretched to a length l_{ds}, $E_{dsDNA}(j_{tot}-j, l_{ds})$, obtained from the introduced tWLC model. Both elastic energy terms depend on material parameters: the Kuhn length L_k and the stretch modulus S_{FJC} for the freely jointed chain model and the persistence length L_p, the stretch modulus S, the twist rigidity C and the twist–stretch coupling $g(F)$. These elastic parameters were determined by fitting the freely jointed chain model to ssDNA and the tWLC model to dsDNA for forces below the overstretching force, as for Fig. 2b. (4) The last energy term represents the potential energy of both microspheres in the harmonic optical traps (Supplementary Information for further detail). Using these energy terms, expectation values and variances of observables are calculated using canonical ensemble averaging[26] over the (j, l_{ss}, l_{ds}) phase space, while applying the boundary condition $l_{ds} + l_{ss} + 2x + d_{bead} = d_{trap}$ (with d_{bead} the microsphere diameter, x the displacement of the microsphere from the trap centre and d_{trap} the distance between the trap centres). In Fig. 4a and b this model is compared to the experimental data, yielding agreement, not only on the force level at which unpeeling occurs (within the estimated force calibration error of ~5%), but also on the location and size of the sequence-specific stick–slip melting bursts. Note that our model using the base-pairing energy determined at zero force predicts the overstretching force of ~65 pN remarkably well. This indicates that at 65 pN the base-pairing energy, with contributions from hydrogen bonding and base-stacking, is not significantly reduced by tension. Furthermore, we did not need to include a kinetic barrier or second transition before final strand separation to describe the unpeeling of DNA by a single melting front (Fig. 4b; Supplementary Fig. S5; refs 27–29). A comparison between theoretically predicted and experimentally observed stalling locations of the unpeeling front for an ensemble (12 independent measurements) is shown in Fig. 4c. In the experimental dwell-time histogram we observe stalling (at 41 locations) at the majority of the 37 theoretically predicted locations. Five stalling locations, predicted by the equilibrium model, show

up only faintly in the dwell-time histogram (discontinuous bars in Fig. 4c). Such events appear to occur after a larger than predicted stalling event, resulting in a reduction of the dwell times owing to the additionally accumulated mechanical energy. Furthermore, nine experimentally observed stalling locations (stars in Fig. 4c) are not captured by the model. These mostly occur close to large melting bursts (for example at $j = \sim$4,200 bp, Fig. 4c) and coincide with peaks in the local stability of the DNA molecule (Fig. 4c, lower panel). Overall, we observed that the correlation between theory and experiment was best in regions with distinct variations in GC–content (for example $j = \sim$0–1,200 bp). Regions with less pronounced features (for example $j = \sim$5,700–6,200 bp) generally show weaker peaks and less agreement with the equilibrium model. We conclude that the overstretching transition can be quantitatively described using an equilibrium thermodynamic model, without introducing any fitting parameters that cannot be determined independently, for all but the largest melting events, with the DNA sequence and elasticity of dsDNA and ssDNA as the only input parameters. This represents an important advance in the quantitative understanding of DNA overstretching by unpeeling. A recent single-molecule study has demonstrated that torsionally relaxed DNA is able to overstretch at 65 pN, even when unpeeling is inhibited by using a specific DNA construct[30]. Hence, unpeeling is the favoured, but not the only overstretching mechanism at this force. It is subject to further investigations whether our equilibrium theory needs modification to describe the alternative overstretching mode, for which the molecular mechanism, at this point, remains elusive.

Finally, we investigated reannealing of the unpeeled DNA on reduction of the distance between the two optical traps (Fig. 1c, inset). Similar to unpeeling, reannealing occurs in bursts (Supplementary Fig. S7A). In contrast to unpeeling, the reannealing patterns vary strongly between experiments. In addition, DNA tension frequently drops below 40 pN during reannealing even at velocities as low as 20 nm s^{-1}. We hypothesized that this hysteresis is due to the formation of secondary structure in the unpeeled ssDNA strand. This secondary structure needs to be resolved, which involves crossing an energy barrier facilitated by thermal fluctuations. The stochastic nature of this process results in a high pausing variability in the reannealing process, causing substantial drops in tension. To support this hypothesis, we determined the local energy stored in the secondary structure of the unpeeled ssDNA strand using MFOLD (ref. 31). These calculations predict regions with enhanced secondary-structure stability, which indeed coincide with locations of prolonged stalls during reannealing (Supplementary Fig. S7B and C).

In summary, in this study we have connected well-defined measurements of the mechanical properties of DNA to a novel, quantitative model. This description covers the full range of forces at which DNA can sustain its double-helical structure and allows structural rearrangements to be followed in great detail. Essential in this model is the inclusion of both the helical structure and the sequence of DNA, two physical features that have a strong impact on protein–DNA interactions[32–34]. The resulting compact expression of the analytical tWLC model can be readily applied to force–extension measurements of DNA and DNA in association with proteins involved in genome transactions. The benefits over currently applied models are threefold: deviations from the Hookean elasticity of DNA at intermediate and high forces can now be attributed to changes in the helicity of DNA. Consequently, it permits a more detailed and accurate distinction between entropic effects covered by the persistence length and enthalpic features such as the stretching modulus, the twist rigidity and the twist–stretch coupling. In addition, it allows quantification of the force-dependence of the twist–stretch coupling $g(F)$, in addition to contour length L_c, stretching modulus S and persistence length L_p (refs 35,36). The analysis of our low-noise measurements of DNA elasticity yields a persistence length of 39 ± 3 nm. This value is somewhat smaller than the established value of ~50 nm (refs 4,37,38), but in agreement with a previous study[2]. Finally, the introduced sequence-dependent mathematical description of force-induced DNA melting allows quantification of the local stabilizing or destabilizing effects of protein binding on dsDNA. To conclude, the deeper understanding of DNA elasticity and mechanical stability presented in this study makes DNA force–extension measurements an even more powerful tool for the investigation of the thermodynamics and structural rearrangements associated with the activity of proteins acting on DNA. Hence, the tWLC model offers a new standard for the investigation of the physical mechanisms of genomic transactions.

Methods

All force–extension measurements were conducted under the following conditions: 10 mM Tris-HCl, pH 7.8, 50 mM NaCl, 20 °C. The visualization of fluorescently labelled RPA was performed using a combined fluorescence and dual-beam optical trapping instrument, which has been described in detail previously[12]. The fluorescent labelling of RPA, along with the experimental procedure for visualizing fluorescent RPA on DNA, was performed as explained in ref. 11. The DNA construct that possesses biotin labels at three ends of the strands was generated as follows. First, two 5′-overhangs were introduced into the circular 8,393 bp plasmid pKYB1 (NEB, Ipswich, USA) using the restriction enzyme EcoRI (Fermentas, Burlington, Canada). The two recessed 3′-ends of this linearized plasmid were biotin labelled by incorporation of biotinylated dATPs (NEB, Ipswich, USA) along with unlabelled dTTPs (Invitrogen, Carlsbad, USA), using Klenow exo$^-$ DNA polymerase (Fermentas, Burlington, Canada). A 3′ overhang was introduced using KpnI (Fermentas, Burlington, Canada), which possesses a single restriction site in this construct. The 8,356 bp fragment was selected and purified. A 29 bp primer possessing four biotinylated nucleotides at the 5′-end (5′-cTcTcTcT ctc ttc tct ctt ctc tt gtac-3′; biotin modifications are depicted with a capital letter) was annealed and ligated to the 3′-overhang of the 8,356 bp fragment using T4 DNA Ligase (Fermentas, Burlington, Canada). The resulting 25 bp 5′-overhang was filled in with biotinylated dATPs along with unlabelled dGTPs, using Klenow exo$^-$ DNA polymerase.

Received 26 November 2010; accepted 13 April 2011; published online 22 May 2011

References

1. Odijk, T. Stiff chains and filaments under tension. *Macromolecules* **28,** 7016–7018 (1995).
2. Wang, M. D., Yin, H., Landick, R., Gelles, J. & Block, S. M. Stretching DNA with optical tweezers. *Biophys. J.* **72,** 1335–1346 (1997).
3. Smith, S. B., Cui, Y. & Bustamante, C. Overstretching B-DNA: The elastic response of individual double-stranded and single-stranded DNA molecules. *Science* **271,** 795–799 (1996).
4. Marko, J. F. & Siggia, E. D. Stretching DNA. *Macromolecules* **28,** 8759–8770 (1995).
5. Gore, J. *et al.* DNA overwinds when stretched. *Nature* **442,** 836–839 (2006).
6. Cluzel, P. *et al.* DNA: An extensible molecule. *Science* **271,** 792–794 (1996).
7. Léger, J. F. *et al.* Structural transitions of a twisted and stretched DNA molecule. *Phys. Rev. Lett.* **83,** 1066–1069 (1999).
8. Wenner, J. R., Williams, M. C., Rouzina, I. & Bloomfield, V. A. Salt dependence of the elasticity and overstretching transition of single DNA molecules. *Biophys. J.* **82,** 3160–3169 (2002).
9. Williams, M. C., Wenner, J. R., Rouzina, I. & Bloomfield, V. A. Entropy and heat capacity of DNA melting from temperature dependence of single molecule stretching. *Biophys. J.* **80,** 1932–1939 (2001).
10. Shokri, L., McCauley, M. J., Rouzina, I. & Williams, M. C. DNA overstretching in the presence of glyoxal: Structural evidence of force-induced DNA melting. *Biophys. J.* **95,** 1248–1255 (2008).
11. van Mameren, J. *et al.* Unraveling the structure of DNA during overstretching by using multicolor, single-molecule fluorescence imaging. *Proc. Natl Acad. Sci. USA* **106,** 18231–18236 (2009).
12. Gross, P., Farge, G., Peterman, E. J. G. & Wuite, G. J. L. Combining optical tweezers, single-molecule fluorescence microscopy, and microfuidics for studies of DNA-protein interactions. *Methods Enzymol.* **475,** 427–453 (2010).
13. Marko, J. F. Stretching must twist DNA. *Europhys. Lett.* **38,** 183–188 (1997).
14. Kamien, R. D., Lubensky, T. C., Nelson, P. & Ohern, C. S. Direct determination of DNA twist–stretch coupling. *Europhys. Lett.* **38,** 237–242 (1997).
15. Marko, J. F. DNA under high tension: Overstretching, undertwisting, and relaxation dynamics. *Phys. Rev. E* **57,** 2134–2149 (1998).
16. Bryant, Z. *et al.* Structural transitions and elasticity from torque measurements on DNA. *Nature* **424,** 338–341 (2003).

17. Sheinin, M. Y. & Wang, M. D. Twist–stretch coupling and phase transition during DNA supercoiling. *Phys. Chem. Chem. Phys.* **11,** 4800–4803 (2009).
18. Lionnet, T., Joubaud, S., Lavery, R., Bensimon, D. & Croquette, V. Wringing out DNA. *Phys. Rev. Lett.* **96,** 1781021–1781024 (2006).
19. Essevaz-Roulet, B., Bockelmann, U. & Heslot, F. Mechanical separation of the complementary strands of DNA. *Proc. Natl Acad. Sci. USA* **94,** 11935–11940 (1997).
20. Bockelmann, U., Essevaz-Roulet, B. & Heslot, F. Molecular stick–slip motion revealed by opening DNA with piconewton forces. *Phys. Rev. Lett.* **79,** 4489–4492 (1997).
21. Bockelmann, U., Thomen, P., Essevaz-Roulet, B., Viasnoff, V. & Heslot, F. Unzipping DNA with optical tweezers: High sequence sensitivity and force flips. *Biophys. J.* **82,** 1537–1553 (2002).
22. Rouzina, I. & Bloomfield, V. A. Force-induced melting of the DNA double helix-1. Thermodynamic analysis. *Biophys. J.* **80,** 882–893 (2001).
23. Liphardt, J., Onoa, B., Smith, S. B., Tinoco, I. & Bustamante, C. Reversible unfolding of single RNA molecules by mechanical force. *Science* **292,** 733–737 (2001).
24. Woodside, M. T. *et al.* Nanomechanical measurements of the sequence-dependent folding landscapes of single nucleic acid hairpins. *Proc. Natl Acad. Sci. USA* **103,** 6190–6195 (2006).
25. SantaLucia, J. A unified view of polymer, dumbbell, and oligonucleotide DNA nearest-neighbour thermodynamics. *Proc. Natl Acad. Sci. USA* **95,** 1460–1465 (1998).
26. Landau, L. & Lifshitz, E. *Statistical Physics* 3rd edn Vol. 5, Part 1 (Butterworth-Heinemann, 1980).
27. Albrecht, C. H., Neuert, G., Lugmaier, R. A. & Gaub, H. E. Molecular force balance measurements reveal that double-stranded DNA unbinds under force in rate-dependent pathways. *Biophys. J.* **94,** 4766–4774 (2008).
28. Clausen-Schaumann, H., Rief, M., Tolksdorf, C. & Gaub, H. E. Mechanical stability of single DNA molecules. *Biophys. J.* **78,** 1997–2007 (2000).
29. Calderon, C. P., Chen, W. H., Lin, K. J., Harris, N. C. & Kiang, C. H. Quantifying DNA melting transitions using single-molecule force spectroscopy. *J. Phys. Condens. Matter* **21,** 034114 (2009).
30. Paik, D. H. & Perkins, T. T. Overstretching DNA at 65 pN does not require peeling from free ends or nicks. *J. Am. Chem. Soc.* **133,** 3219–3221 (2011).
31. Zuker, M. Mfold web server for nucleic acid folding and hybridization prediction. *Nucleic Acids Res.* **31,** 3406–3415 (2003).
32. Nollmann, M. *et al.* Multiple modes of Escherichia coli DNA gyrase activity revealed by force and torque. *Nat. Struct. Mol. Biol.* **14,** 264–271 (2007).
33. Hall, M. A. *et al.* High-resolution dynamic mapping of histone-DNA interactions in a nucleosome. *Nat. Struct. Mol. Biol.* **16,** 124–129 (2009).
34. Revyakin, A., Revyakin, A., Ebright, R. H. & Strick, T. R. Abortive initiation and productive initiation by RNA polymerase involve DNA scrunching. *Science* **314,** 1139–1143 (2006).
35. McCauley, M. J. & Williams, M. C. Review: Optical tweezers experiments resolve distinct modes of DNA-protein binding. *Biopolymers* **91,** 265–282 (2009).
36. Hegner, M., Smith, S. B. & Bustamante, C. Polymerization and mechanical properties of single RecA-DNA filaments. *Proc. Natl Acad. Sci. USA* **96,** 10109–10114 (1999).
37. Baumann, C. G., Smith, S. B., Bloomfield, V. A. & Bustamante, C. Ionic effects on the elasticity of single DNA molecules. *Proc. Natl Acad. Sci. USA* **94,** 6185–6190 (1997).
38. Bustamante, C., Marko, J. F., Siggia, E. D. & Smith, S. Entropic elasticity of lambda-phage DNA. *Science* **265,** 1599–1600 (1994).

Acknowledgements

We thank J. Gore for communicating his experimental data. We thank M. Depken and C. Broederz for discussions. We thank M. Modesti for the kind gift of the eGFP labelled RPA. This work is part of the research program of the 'Stichting voor Fundamenteel Onderzoek der Materie (FOM)', which is financially supported by the 'Nederlandse Organisatie voor Wetenschappelijk Onderzoek (NWO)' (N.L., E.J.G.P., G.J.L.W.). P.G. is supported by ATLAS, a European Commission-funded Marie Curie early stage training network. G.J.L.W. is recipient of a VICI grant from the 'Nederlandse Organisatie voor Wetenschappelijk Onderzoek (NWO)'. U.B. was supported by a KNAW visiting professor grant.

Author contributions

P.G. performed experiments, the DNA unwinding modelling and analysis. N.L. performed the DNA unwinding analysis. L.B.O. assisted in the design of the study. U.B. developed the thermodynamical model for DNA unpeeling and assisted in the design of the study. E.J.G.P. and G.J.L.W. designed the study and assisted with the analysis. All the authors contributed to the writing of the paper.

Additional information

The authors declare no competing financial interests. Supplementary information accompanies this paper on www.nature.com/naturephysics. Reprints and permissions information is available online at http://www.nature.com/reprints. Correspondence and requests for materials should be addressed to E.J.G.P. or G.J.L.W.